CrystEngComm

Cite this: *CrystEngComm*, 2012, **14**, 5305–5314

www.rsc.org/crystengcomm

PAPER

Binding discrepancy of fluoride in quaternary ammonium and alkali salts by a tris(amide) receptor in solid and solution states†‡

Sandeep Kumar Dey, Barun Kumar Datta and Gopal Das*

Received 18th April 2012, Accepted 3rd June 2012
DOI: 10.1039/c2ce25592h

A dinitrophenyl functionalized tris(amide) receptor, **L**, showed distinct complexation behaviour towards the F^- anion when tetrabutylammonium fluoride (TBAF) and potassium fluoride (KF) salts were individually employed for the recognition of F^- with **L**. X-ray crystallography analyses revealed the formation of a F^-–encapsulated complex (1 : 1 host–guest) stabilized by three N–H···F^- and three C–H···F^- hydrogen bonds when TBAF was employed as the F^- source, whereas in the KF complex of **L** (1 : 1 host–guest), the receptor is involved in side-cleft binding of a hydrated KF contact ion-pair governed by amide N–H···F^-, aryl C–H···F^- and lp(F^-)···π interactions. The binding of hydrated KF is identical to the side-cleft binding of solvents such as DMSO and DMF *via* N–H···O, aryl C–H···O and lp(O) ···π interactions, which has been exemplified by X-ray crystallography and a detailed Hirshfeld surface analyses of the crystals. The binding discrepancy of F^- in the TBAF and KF complexes of **L** has also been manifested in the solution state by ^{1}H NMR and 2D NOESY NMR experiments. In the ^{1}H NMR analyses, a huge downfield shift of the coordinating –NH and *ortho*–CH protons was observed in the TBAF complex in comparison to the KF complex whereas, in the 2D NOESY NMR experiments, a disappearance of the signals corresponding to the through-space NOE coupling between the –NH and *ortho*–CH protons was observed in the former when compared to the latter and free receptor, **L**.

Introduction

The importance of supramolecular interactions in nature has been increasingly recognized in recent years and thus, enormous efforts have been put forward by researchers to gain a better insight and understand the ion-specific interaction of certain functionalities in abiotic receptors.[1] This has led to an exponential growth of studies in the area of molecular recognition with varying binding motifs appended on a suitable platform. The field of anion receptor chemistry continues to expand with new synthetic hosts capable of recognizing anions with environmental and biomedical relevance.[2] It has already been established that, apart from the charge density of the anionic species, the spatial arrangement of the binding motif(s) in the receptor and geometry of the anions is also crucial in influencing the receptor–anion binding efficiency and specificity. Among anionic analytes, the recognition and sensing of fluoride is an area of immense interest to the chemical society due to its diverse role in industry, food and toxicity.[3] Due to its high electronegativity and high hydration enthalpy, fluoride exists as various types of fluoride–water clusters (the hydrated form) in water or in presence of moisture and thus, its recognition by abiotic receptors becomes a challenging task.[4] Furthermore, receptors for anions such as fluoride should target the hydrated alkali metal salts rather than the quaternary ammonium salts because in nature, fluoride exists mostly as its Na/K salts (minerals such as villiaumite and carobbiite). On the other hand, self-assembled supramolecular capsules that provide an isolated nanocavity have attracted much attention in recent years for unusual guest encapsulation.[5] Within the area of self-assembly driven by hydrogen bonding, numerous molecular capsules have been constructed by different laboratories *via* the self-assembly

Department of Chemistry, Indian Institute of Technology Guwahati, Assam, 781 03, India. E-mail: gdas@iitg.ernet.in; Fax: +91-361-258-2349; Tel: +91-361-258-2313

† Electronic supplementary information (ESI) available: X-ray crystallographic file of the structures in CIF format, selected non-covalent interactions, crystal packing networks, ^{1}H and ^{13}C spectra. CCDC reference numbers 761161–76113. For ESI and crystallographic data in CIF or other electronic format see DOI: 10.1039/c2ce25592h

‡ Crystal data for **1d**: Fw = $C_{46}H_{60}FN_{11}O_{16}$, M = 1042.05, CCDC = 761161, T = 298(2) K, triclinic, space group $P\bar{1}$, a = 10.1372(3), b = 16.4160(5), c = 17.3515(8) Å, α = 109.413(2)°, β = 97.059(2)°, γ = 106.906(1)°, V = 2527.35(17) Å^3, Z = 2, μ = 0.107 mm^{-1}, 9814 unique reflections, 7233 observed , $R(F)$ = 0.0645 ($I > 2\sigma(I)$), $wR(F^2)$ = 0.2429 (all data), GOF (F^2) = 1.005. Crystal data for **2**: Fw = $C_{27}H_{24}FKN_{10}O_{17}$, M = 1858.21, CCDC = 761162, T = 298(2) K, triclinic, space group $P\bar{1}$, a = 11.2710(12), b = 12.4543(13), c = 12.8718(14) Å , α = 84.825(6)°, β = 79.744(6)°, γ = 88.329(6)°, V = 1770.6(3) Å^3, Z = 2, μ = 0.246 mm^{-1}, 7784 unique reflections, 6870 observed, $R(F)$ = 0.0838 ($I > 2\sigma(I)$, $wR(F^2)$ = 0.2728 (all data), GOF (F^2) = 1.035. Crystal data for **L**·DMF: Fw = $C_{30}H_{31}N_{11}O_{16}$, M = 801.66, CCDC = 761163, T = 298(2) K, monoclinic, space group $P2_1/c$, a = 17.2139(6), b = 11.1890(3), c = 25.1968(7) Å ,α = 90.00° β = 131.890(2)° γ = 90.00°, V = 3612.8(2) Å^3, Z = 4, μ = 0.122 mm^{-1}, 8991 unique reflections, 4777 observed, $R(F)$ = 0.0580 ($I > 2\sigma(I)$, $wR(F^2)$ = 0.2115 (all data), GOF (F^2) = 1.023.

of various hydrogen bonding motifs such as calixarenes, resorcinarenes, glycoluril and tripodal derivatives, mostly in the presence of a neutral or ionic guest species.[6]

Furthermore, as anions display a wide range of geometries, the directionality of the hydrogen bonds is frequently utilized to achieve complementarity between the designed receptors and target anion(s). Artificial receptors mostly utilize N–H···anion hydrogen bonds whereas C–H···anion and anion···π interactions are rarely utilized for the recognition/sensing of anions even though they play an important role in nature.[7] More recently, C–H···anion and anion···π interactions have been independently employed by Das and Saha *et al.* for the selective sensing of the F^- ion, based on an appropriate receptor–chromophore format that showed an enhanced F^- binding affinity.[8] Increasing evidence of these interactions comes in the form of the direct observation of close contacts in crystallographic structures, anion-induced chemical shifts of C–H protons in NMR spectra and theoretical calculations.[9] Although the binding of anionic guests within pre-organized macrocyclic systems is relatively straightforward to understand, the binding processes of flexible podand receptors remain more elusive. In this context, a recent theoretical investigation by Hay *et al.* and several structural reports on anion complexes of multi-armed receptors showed that the effect of electron withdrawing substituents on the aryl terminals significantly enhances the stability of anion complexes.[10] Although, acyclic podand receptors with multi-armed functionality have been shown to be effective systems for the binding of a variety of anions, their uses as selective fluoride binding hosts are barely known.

In our recent communication, we have shown that the dinitrophenyl functionalized tris(amide) receptor, **L**, (Scheme 1) behaves as a selective chemosensor for the fluoride ion *via* encapsulation of the anion within the tripodal scaffold in a library of polar aprotic solvents, exhibiting solvatochromism and solvatomorphism (TBA[**L**(F)]·H_2O (**1a**), TBA[**L**(F)]·DMF (**1b**) and TBA[**L**(F)]·THF (**1c**) solvates).[11] In a continuation of our previous effort, herein we report the acetone solvate of the F^-–bound receptor capsule (TBA[**L**(F)]·$(CH_3)_2CO$, **1d**), prepared in an acetone–ethyl acetate media and the solvent-specific crystallization of the KF complex of **L** ([**L**·KF$(H_2O)_2$], **2**) from an acetonitrile media, where a hydrated KF contact ion-pair is coordinated to the receptor molecule(s) *via* N–H···F^-, C–H···F^- and lp(F^-)···π interactions. The attempted crystallization of the 1 : 1 KF complex (**2**) in solvents such as DMSO and DMF yielded the respective solvates of the ligand, where the lattice solvent interacts with the receptor molecules *via* N–H···O, C–H···O and lp(O) ···π interactions involving the oxygen atom of the respective lattice solvents. The structural similarities between complex **2** and the solvatomorphs of **L** have also been accounted for in terms of Hirshfeld surface analyses of the crystals which show the presence of identical supramolecular interactions, as observed in the single-crystal X-ray crystallography analyses. The binding discrepancy of F^- in complexes **1d** and **2** has also been demonstrated in the solution state by ^{1}H NMR and 2D NOESY NMR experiments.

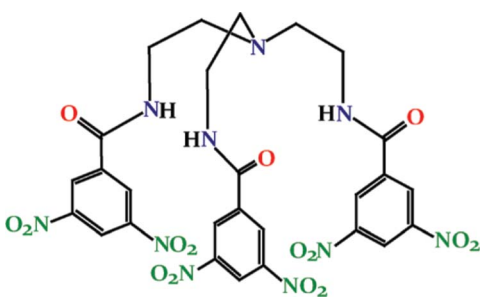

Scheme 1 Molecular structure of the tris(amide) receptor, **L**.

Experimental section

Materials and methods

All reagents and solvents were obtained from commercial sources and used as received without further purification. Tris(2-aminoethyl)amine, (tren) and 3,5-dinitrobenzoyl chloride were purchased from Sigma-Aldrich and used as received. Tetrabutylammonium fluoride and potassium fluoride salts were purchased from Merck-India and used as received. The ^{1}H NMR and 2D NOESY NMR spectra were recorded on a Varian FT-400 MHz instrument and the chemical shifts were recorded in parts per million (ppm) using tetramethylsilane (TMS) or a residual solvent peak as a reference. The FT-IR spectra were recorded on a Perkin-Elmer-Spectrum One FT-IR spectrometer with KBr disks in the range of 4000–450 cm^{-1}.

X-ray crystallography

In each case, a crystal of suitable size was selected from the mother liquor and immersed in silicone oil. It was then mounted onto the tip of a glass fiber and cemented using epoxy resin. The intensity data was collected using a Bruker SMART APEX-II CCD diffractometer, equipped with a fine focus 1.75 kW sealed tube using Mo–Kα radiation (λ = 0.71073 Å) at 180 or 298 K, with increasing ω (width of 0.3° per frame) at a scan speed of 5 s $frame^{-1}$. SMART software was used for the data acquisition. Data integration and reduction was undertaken with SAINT and XPREP[12] software. Multi-scan empirical absorption corrections were applied to the data using the SADABS program.[13] The structures were solved by direct methods using SHELXS-97[14] and refined with full-matrix least-squares on F^2 using SHELXL-97.[15] All non-hydrogen atoms were refined anisotropically. Hydrogen atoms attached to all carbon atoms were geometrically fixed and the positional and temperature factors were refined isotropically. Structural illustrations have been drawn with MERCURY-2.3[16] for Windows.

Synthesis and characterization

Receptor L. The tripodal amide receptor, **L**, was synthesized following our recent report where the reaction of tris(2-aminoethyl amine) with 3,5-dinitrobenzoyl chloride in a 1 : 3 molar ratio at room temperature yielded **L** in high yield (75%) and the characterization data matched with the recently published data.[11] m.p: 252 °C; ^{1}H NMR (DMSO-d_6, 400 MHz) δ (ppm) 2.84 (s, 6H, NCH_2), 3.48 (d, 6H, CONH–CH_2), 8.88 (d, 3H, *para*-ArCH), 8.91 (s, 6H, *ortho*-ArCH), 9.15 (s, 3H, amide–NH); ^{13}C NMR (100 MHz, DMSO-d_6): δ 45.73 (×3C, –NCH_2), 53.08 (×3C, CONH–CH_2), 120.58 (×3C, ArH),

127.35 (×6C, ArH), 137.06 (×3C, ArH), 148.01 (×6C, ArH), 162.20 (×3C, C=O); FT-IR (ν, cm^{-1}) 1346 (*asym.*, NO_2), 1540 (*sym.*, NO_2), 1670 (C=O), 3088 (C–H), 3428 (N–H).

Complex TBA[L(F)]·$(CH_3)_2CO$, (1d). Complex **1d** was prepared by adding an excess (10 equiv.) of tetrabutylammonium fluoride (TBAF) into a suspension of **L** (370 mg, 0.5 mmol) in 15 mL of an acetone–ethyl acetate (2 : 1) binary solvent mixture. After the addition of the TBAF salt, the mixture was stirred for approximately 15 min at RT during which the suspension turned clear. Finally, the resulting purple coloured solution was filtered in a test-tube and allowed to slowly evaporate below 10 °C in a refrigerator. Light pink crystals of **1d** suitable for single crystal X-ray analysis were obtained within 7 days. Yield: 42–45% based on **L**. It is worth mentioning that our previous efforts to obtain single crystals of **1d** at RT were unsuccessful. However, RT crystallization of the receptor–fluoride complex can reproducibly be accomplished from other aprotic solvents *viz*, MeCN, THF and DMF, which yielded the respective solvates of TBA[**L**(F)].[11] ^{1}H NMR (DMSO-d_6, 400 MHz) δ (ppm) 0.92 (t, 12H, TBA-CH_3), 1.30 (q, 8H, TBA-CH_2), 1.56 (t, 8H, TBA-CH_2), 1.98 (s, 6H, $(CH_3)_2CO$) 2.61 (s, 6H, NCH_2), 3.16 (t, 8H, TBA-N^+CH_2), 8.80 (s, 3H, *para*-ArCH), 9.60 (s, 6H, *ortho*-ArCH), 12.49 (s, 3H, amide-NH); ^{13}C NMR (DMSO-d_6, 100 MHz) δ (ppm) 13.48 (×4C, TBA-CH_3), 19.22 (×4C, TBA-CH_2), 23.08 (×4C, TBA-CH_2), 38.30 (×3C, –NCH_2), 57.56 (×3C, CONH-CH_2), 79.19 (×4C, TBA-N^+CH_2), 120.21 (×3C, ArH), 128.17 (×6C, ArH), 137.59 (×3C, ArH), 147.95 (×6C, ArH), 162.23 (×3C, C=O); FT-IR (ν, cm^{-1}) 1343 (*asym.*, NO_2), 1538 (*sym.*, NO_2), 1645 (C=O), 2962(C–H), 3421 (N–H).

Complex [L·KF$(H_2O)_2$], 2. Complex **2** was prepared by adding an equivalent amount of a potassium fluoride solution in water (1 ml) into a suspension of **L** (370 mg, 0.5 mmol) in 20 mL of acetonitrile. After the addition of the KF salt, the suspension was stirred for approximately an hour at 60 °C under reflux. The resulting solution which was thus obtained was filtered into a test-tube and allowed to slowly evaporate at RT for crystallization. Red crystals of **2**, suitable for single crystal X-ray analysis, were obtained within 10–12 days. Yield: 28–30% based on **L**. It is worth mentioning that room temperature crystallization of **L** in the presence of an equivalent amount of KF in other aprotic solvents such as DMSO and DMF were unsuccessful in obtaining the complex and yielded the respective solvates of the ligand. ^{1}H NMR (DMSO-d_6, 400 MHz) δ (ppm) 2.70 (s, 6H, NCH_2), 8.83 (s, 3H, *para*-ArCH), 9.19 (s, 6H, *ortho*-ArCH). Due to the poor solubility of the isolated crystals of **2** in deuterated solvents such as CD_3CN and DMSO-d_6, the ^{13}C NMR spectrum could not be recorded. FT-IR (ν, cm^{-1}) 1342 (*asym.*, NO_2), 1537 (*sym.*, NO_2), 1646 (C=O), 2921 (C–H), 3254 and 3354 (N–H).

Results and discussion

Crystal structure analyses

Receptor **L** possesses a highly organized tripodal scaffold with hydrogen bond-donating amide functions suitable for anion binding and encapsulation. In addition, functionalizations of **L** with π-acidic dinitrophenyl aryl terminals significantly enhance the binding ability of the receptor towards anionic guests. The chelate-effect may also play an important role in the anion binding affinity because of the favourable contributions from both entropy and enthalpy. From the perspective of the anion receptor chemistry, crystallization has traditionally been a route to understand the structural insights of the anion complexes formed, primarily by single-crystal X-ray diffraction (XRD) analysis which are then related to the observed binding in solution using mostly NMR spectroscopy.

Complex TBA[**L**(F)]·$(CH_3)_2CO$, **1d** crystallizes in the triclinic space group $P\bar{1}$ with $Z = 2$ and an acetone molecule from the solvent of crystallization. The crystal structure analysis shows that a fluoride ion is bound within the receptor scaffold and governed by six hydrogen bonds from the amide-NH functions and three aryl-CH protons (*ortho*) of the π-acidic receptor, resulting in an anion entrapped unimolecular capsule (Fig. 1a). The encapsulated F^- ion is N–H···F^- hydrogen bonded to the three amide protons with an average contact distance of 2.685 Å whereas the coordinating *ortho*-aryl protons interact through C–H···F^- hydrogen bonds with an average distance of 2.965 Å, demonstrating the strong binding of F^- by **L** in the solid state (Table 1). A correlation of the D–H···F^- distance *vs.* the D–H···F^- angle reveals that hydrogen bonds formed between the encapsulated F^- ion with the six coordinating donor atoms are in the strong hydrogen bonding interaction region with donor-to-acceptor (D···F) distances ranging from 2.662 to 3.022 Å and D–H···F angles ranging from 143(2)° to 179(3)° (Table 1). Intermolecular short contact analysis shows the dimeric association of two F^--encapsulated receptor units with opposite orientation by aryl C–H···O and nitro–nitro interactions.

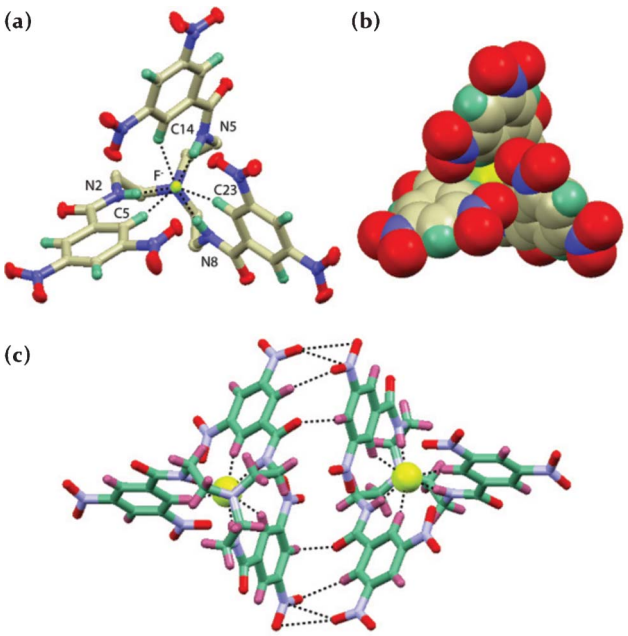

Fig. 1 (a) X-ray structure of **1d** showing the encapsulation of F^- inside the receptor scaffold, where the dotted lines represent (D–H)···F^- interactions; (b) Spacefill representation depicting the formation of an F^--encapsulated neutral molecule capsule in **1d**; (c) Dimeric association of two F^--encapsulated receptor units by aryl C–H···O and nitro–nitro n→π*(k) interactions. The TBA cation and the solvent are omitted for clarity.

Table 1 Hydrogen bond interactions involved in the crystal structures of **L**·DMF, **1d** and **2**

Crystals	D–H···A	*d* (H···A)	*d* (D···A)	< (DH···A)
[**L**·DMF]				
Intraligand interactions	N2–H···O11	2.12(2)	2.973(3)	171(1)
	C9–H···O11	2.46(2)	3.308(3)	151(2)
	C2g···C3g	—	3.830	—
Interactions with DMF	N8–H···O16	2.04(2)	2.846(3)	154(2)
	C23–H···O16	2.42(2)	3.337(3)	165(2)
	C30–H···O6	2.64(2)	3.504(6)	154(2)
	O16···C3g	—	3.429	—
Interligand interactions	N5–H···O1	2.17(2)	2.912(3)	144(1)
	C2–H···O10	2.59(2)	3.076(5)	111(2)
	C11–H···O8	2.63(2)	3.298(4)	126(2)
	C10–H···O9	2.68(2)	3.530(3)	146(2)
	C19–H···O15	2.69(2)	3.420(3)	132(2)
	O12···C21	—	3.218(6)	—
	O13···C6	—	3.182(3)	—
[**L**·KF(H_2O)$_2$] (**2**)				
Intraligand interactions	N2–H···O6	2.04(2)	2.904(3)	174(2)
	C9–H···O6	2.46(2)	3.188(4)	134(2)
	C2g···C3g	—	3.750	—
Interactions of KF(H_2O)$_2$	N5–H···F1	2.00(3)	2.841(4)	163(2)
	C14–H···F1	2.34(2)	3.240(4)	160(2)
	F1···C2g	—	3.527	—
Interligand interactions	N8–H···O1	2.09(2)	2.860(3)	147(2)
	C1–HA···O3	2.61(4)	3.274(5)	125(2)
	C1–HB···O3	2.65(4)	3.522(6)	149(2)
	C2–H···O13	2.67(4)	3.134(6)	110(2)
	C19–H···O1	2.71(2)	3.432(4)	131(2)
	O2···N9	—	2.983(4)	—
	O14···N11	—	3.068(5)	—
	O8···C6	—	3.153(5)	—
	O8···C12	—	3.509(4)	—
TBA[**L**(F)]·(CH_3)$_2$CO (**1d**)				
Interactions with F^-	N2–H···F1	1.77(3)	2.662(3)	170(3)
	N5–H···F1	1.78(2)	2.680(2)	179(2)
	N8–H···F1	1.82(2)	2.713(2)	173(2)
	C5–H···F1	2.12(1)	3.022(3)	162(2)
	C14–H···F1	2.15(1)	2.949(2)	143(2)
	C23–H···F1	2.09(2)	2.925(4)	164(2)
Interligand interactions	C16–H···O1	2.39(2)	3.252(4)	154(2)
	C9–H···O9	2.51(3)	3.427(4)	169(2)
	C20–HA···C27	2.79(3)	3.495(4)	129(2)
	O5···N7	—	2.939(4)	—
	C21···C21	—	3.350(4)	—
	O15···C3	—	3.058(3)	—
	O11···C6	—	3.068(4)	—
	O11···N3	—	2.974(3)	—
Interactions with TBA^+	C30–HB···O1	2.46(2)	3.425(4)	172(2)
	C32–HA···O4	2.61(2)	3.530(3)	157(2)
	C34–HA···O4	2.65(2)	3.555(3)	154(2)
	C37–HB···O4	2.67(2)	3.534(4)	148(2)
	C28–HA···O6	2.44(2)	3.343(4)	154(2)
	C41–HA···O6	2.57(1)	3.528(3)	166(2)
	C31–HB···O8	2.69(2)	3.558(3)	150(2)
	C28–HB···O9	2.40(2)	3.269(4)	148(2)
	C36–HA···O9	2.44(2)	3.317(3)	150(2)
	C42–HA···O10	2.47(2)	3.254(4)	137(2)
	C34–HB···O14	2.67(2)	3.512(4)	144(2)

The C9H and C16H aryl protons from each receptor unit of the dimer are hydrogen bonded to the O9 (nitro oxygen) and O1 (amide oxygen) oxygen atoms, respectively of the other unit whereas the nitro groups are involved in n→π*(k) interactions (Fig. 1c). Two such dimers are interlinked with one another *via* aliphatic C–H···π interactions, n→π* (O:→N C^{-1}) interactions, where the lone pair on the oxygen is added to the N=O or C=O double or partially double bonds, and C:→C contacts occurring as π→π* interactions between the C=O functions of adjacent dimeric units (ESI†). Similar n→π*/n→π*(k) and π→π* electron donor–acceptor interactions have recently been revealed by Gilli *et al.* towards controlling the crystal packing of picric acid and it's adducts with nitrogen bases.[17] Expansion through intermolecular hydrogen bonds generates a 1D chain of F^--entrapped receptor capsules along the crystallographic *b*-axis.

Complex [**L**·KF(H_2O)$_2$], **2**, crystallizes in the $P\bar{1}$ triclinic space group with $Z = 2$. Structural elucidation reveals that the receptor unit is conformationally locked due to intramolecular hydrogen

bonding between the receptor side arms involving N–H···O, C–H···O and π···π interactions, where the amide oxygen O6 is involved in bifurcated hydrogen bonding with the amide proton N2H and aryl hydrogen C9H from the same receptor side arm (N2···O6 = 2.904(3) Å; C9···O6 = 3.188(4) Å). Complementary N–H···O and C–H···O hydrogen bonding between two arms of the receptor presumably assists one of the aryl functions of the intramolecularly hydrogen bonded tripodal arms to be in closer proximity with the aryl ring of the third side arm, resulting in a significant face-to-face interaction (C2g···C3g = 3.750 Å). Structural elucidation further reveals that KF is bound as a contact ion-pair (K^+–F^- = 1.494(3) Å) by **L** where K^+ is coordinated to two water molecules (K^+–O18 = 1.788(5) Å and K^+–O19 = 1.778(6) Å). The strong K^+–F^- ionic interaction that results from the much higher charge density of K^+ (as compared to TBA^+) is certainly of high importance in disabling the expected "encapsulating mode" of the fluoride recognition. Notably, the K^+–F^- bond length in **2** is distinctly shorter when compared to those of anhydrous KF,[18] which exhibits a KF_6 octahedron with a K^+–F^- bond length of 2.674 Å, and $KF{\cdot}2H_2O$[19] having a $K(H_2O)_4(F)_2$ octahedron with a K^+–F^- bond length of 2.716 Å. Furthermore, each hydrated KF contact ion-pair is hydrogen bonded to two adjacent receptor molecules *via* amide N–H···F^-, aryl C–H···F^- and lp(F^-)···π interactions (N5···F1 = 2.841(4) Å; C14···F1 = 3.240(4) Å and F1···C2g = 3.527 Å), resulting in the dimeric association of the receptor molecules bridged by two coordinated $KF(H_2O)_2$ moieties (Fig. 2a). Expansion through hydrogen bonds shows that two such dimeric units are further associated with each other by amide N–H···O and aliphatic C–H···O interactions (N8···O1 = 2.860(3) Å, C19···O1 = 3.432(4) Å, C19···O2 = 3.622(6) Å and C2···O13 = 3.134(6) Å), resulting in a 1D chain of inversely oriented receptor molecules in association with hydrogen bonded $KF(H_2O)_2$ moieties diagonally along the *a*-axis (Fig. 2b). Furthermore, two such 1D chains are interlinked among themselves by multiple C–H···O and n→π* (O:→N C^{-1}) interactions which eventually govern the overall packing of the crystal (ESI†).

The DMF solvate of the receptor **L** (**L**·DMF) crystallizes in the $P2_1/c$ triclinic space group with $Z = 4$. Structural elucidation of **L**·DMF reveals that the combined effect of intramolecular hydrogen bonding and aromatic π···π stacking resists the open conformation of the receptor, as observed in **2**. The amide hydrogen N2H and an aryl proton C9H from the same receptor side arm (involving C1–C9) is intramolecularly hydrogen bonded to the amide oxygen O11 of another arm (involving C10–C18) *via* N–H···O and C–H···O interactions, respectively (N2···O11 = 2.973(3) Å and C9···O11 = 3.308(3) Å), whereas the aryl function C3g of the third arm (involving C19–C27) is involved in an aromatic face-to-face interaction with the ring C2g, attached to the amide function involving oxygen O11 (C3g···C2g = 3.830(3) Å). Short contact analyses (D···A < 4.0 Å) of the crystal structure further shows that the DMF oxygen (O16) is hydrogen bonded to the amide proton N8H (N8···O16 = 2.846(3) Å) and aryl hydrogen C23H (C23···O16 = 3.337(3) Å) from the same flexible side arm (involving C19–C27) of the receptor and also interacts with the π-acidic aryl function C3g, involving the identical side arm of an adjacent receptor unit *via* an lp(O) ···π interaction (O16···C3g = 3.429 Å). Additionally, the carbonyl hydrogen (C30H) of the lattice DMF interacts with

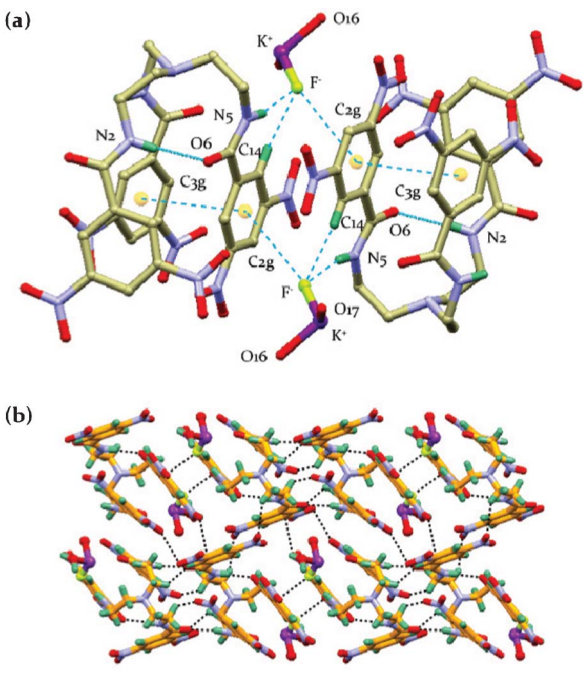

Fig. 2 (a) X-ray structure of complex **2** showing the intramolecular hydrogen bonding and interactions with the $KF(H_2O)_2$ adduct; (b) Crystal packing of **2**, as viewed down the *a*-axis, showing the H-bonding and electron donor–acceptor interactions between two adjacent 1D chains of the receptor molecules.

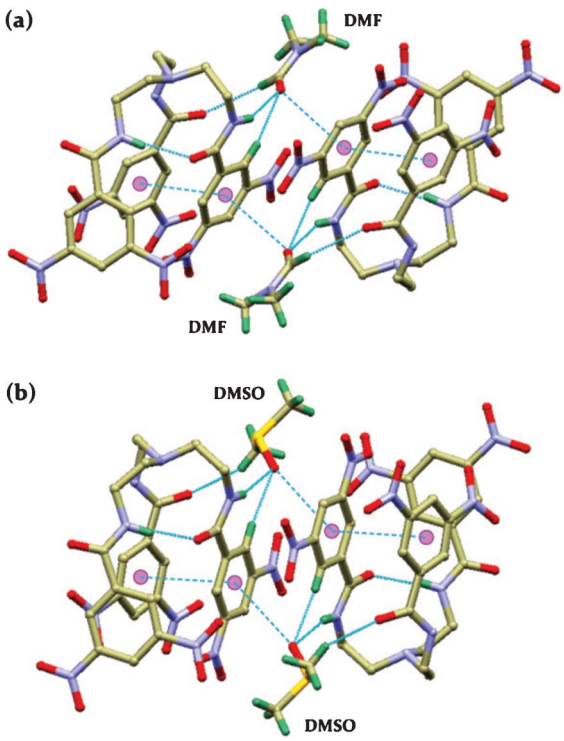

Fig. 3 X-ray structures of the solvatomorphs of **L** showing the identical modes of intramolecular H-bonding and interactions with the lattice solvent molecule in (a) **L**-DMF and (b) **L**-DMSO.

the amide oxygen O6 (C30···O6 = 3.504(4) Å), resulting in a hydrogen bonded dimer formation with two DMF molecules and two molecules of **L** (Fig. 3a). Each solvent bridged dimer is in association with the adjacent dimeric unit *via* a strong N–H···O hydrogen bond that involves an interaction between the amide proton N5H and the amide oxygen O1 of two neighboring dimers (N5···O1 = 2.912(3) Å). The hydrogen bonded association of solvent bridged dimers is further stabilized by two aliphatic C–H···O interactions in which the methylene protons C2H(B) and C10H(B) from two different arms of a receptor dimer make contacts with the nitro oxygen O10 and amide oxygen O1 of another dimeric unit (C2···O10 = 3.076(5) Å and C10···O1 = 3.501(4) Å), resulting in a 1D chain of oppositely oriented receptor units along the *c*-axis (ESI†). However, the overall packing of the crystal is additionally governed by three aliphatic C–H···O (nitro) interactions and n→π* (O:→C) interactions, where the lone pair on the oxygen from the nitro group is added to the C=C or C=O double or partially double bonds,[17] resulting in the formation of a hydrogen bonded sheet-like structure when viewed down the crystallographic *b*-axis (ESI†). The details of the hydrogen bonds involved in the crystal structure of **L**·DMF are provided in Table 1.

Similar types of intra- and intermolecular hydrogen bonding has previously been observed in the DMSO solvate of **L**, where the DMSO oxygen atom is hydrogen bonded to an amide-NH function and an aryl-CH proton (*ortho*) from the same flexible side arm of the receptor and interacts significantly with the π-acidic aryl function involving the identical side arm of an adjacent receptor unit *via* an lp(O) ···π interaction (Fig. 3b and ESI†). The details of the hydrogen bonds involved in the crystal structure of **L**·DMSO are provided in Table S2 in the ESI.†

Thus, from the experimental conditions and structural elucidation, it is obvious that, irrespective of the solvent of crystallization, F^- is encapsulated and bound within the tripodal scaffold by six strong hydrogen bonds from the amide-NH and three aryl-CH functions when the TBAF salt was employed as the primary source of the F^- ion. However, when KF was used as the source for the complexation of the F^- ion by **L**, it has been crystallographically observed that a receptor molecule is involved in the side-cleft binding of the hydrated KF contact ion-pair by an amide N–H···F^- and an aryl C–H···F^- interaction from the same tripodal side arm of the receptor and interacts significantly with the neighbouring $KF(H_2O)_2$ moiety *via* an lp(F^-)···π interaction. Furthermore, the crystallization of the KF complex (**2**) is solvent specific and formed only in an acetonitrile (MeCN) media. Complexation of KF in other aprotic solvents such as DMSO and DMF were not fruitful and resulted in the exclusive crystallization of the respective solvates of **L**, as confirmed by the ^{1}H NMR and FT-IR analyses of the isolated crystals. This can be rationalized in terms of the hydrogen bonding interactions where solvents such as DMSO and DMF are highly capable of competing for the amide-NH functions and π-acidic arenes and thereby disfavour the formation of complex **2**. This scenario is, however, clear from the X-ray crystallographic observation where similar modes of supramolecular interactions have been observed in the crystals of **2** and the DMSO/DMF solvates of **L**. Notably, the DMSO/DMF oxygen atom is involved in amide N–H···O, aryl C–H···O and lp(O) ···π interactions from the same tripodal side arm of two adjacent receptor molecules, which has also been observed in complex **2** involving the F^- atom of the $KF(H_2O)_2$ moiety in replacement of the DMSO or DMF oxygen. It is important to mention here that complex **2** and the previously reported crystal of **L**·DMSO[11] are isostructural, which is evident from the identical unit cell parameters and simulated PXRD patterns.

The binding discrepancy of F^- in complexes **1d** and **2** has also been established by FT-IR analysis (Fig. 4). In the case of the free receptor, the amido carbonyl (NH–C=O) stretching frequency is observed at 1670 cm^{-1} and the N–H stretching frequency is observed at 3428 cm^{-1}. However, in complex **1d** the –C=O stretching vibration is observed at 1645 cm^{-1}, showing a considerable shift of 25 cm^{-1} relative to the free **L** and the N–H peak is significantly broadened due to the formation of strong N–H···F^- hydrogen bonds with the encapsulated F^- anion, as evident from the crystal structure of **1d**. However, in complex **2**, the –C=O stretching vibration experiences an observable shift of 24 cm^{-1} relative to the free **L** and the peak for the N–H stretching is split into two distinct peaks at 3254 and 3354 cm^{-1}, indicating the existence of two different types of hydrogen bonded N–H protons (N–H···O and N–H···F^-), as observed in the crystal structure of **2**.

Hirshfeld surface analyses. The structural similarities between complex **2** and the DMSO or DMF solvates of **L** have also been visualised by Hirshfeld surface analysis, which is a useful tool to describe the surface characteristics of molecules.[20] Hirshfeld surfaces offer a novel way of visualizing intermolecular interactions by colour-coding short or long contacts and two-dimensional fingerprint plots complement these surfaces, quantitatively summarizing the nature and type of intermolecular interactions experienced by the molecules in the crystal as "contact contribution".

Fig. 5 displays the Hirshfeld surfaces of the receptor unit mapped with d_{norm} for solvated **L** and complex **2** and highlights the intermolecular N–H···O interactions as bright red spots and

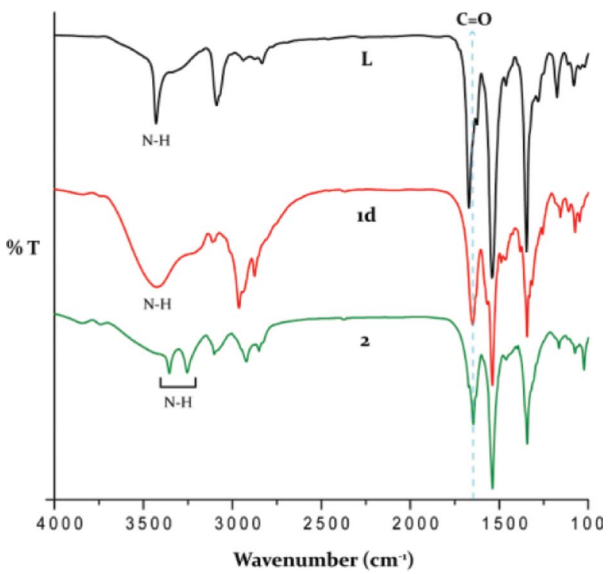

Fig. 4 Overlay FT-IR spectra of the free receptor, **L**, and complexes **1d** and **2**.

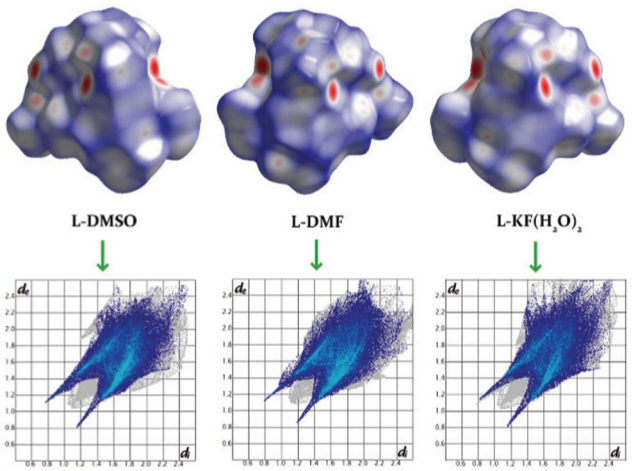

Fig. 5 Hirshfeld surface analysis of **L**·DMSO, **L**·DMF and complex **2**, showing the d_{norm} surfaces of the respective receptor unit and the corresponding 2D fingerprint plots with the H···O interactions highlighted in blue colour.

C–H···O interactions as bright to faint red spots that exist between the adjacent receptor molecules and between a tripodal side arm of the receptor with the lattice solvent in the solvatomorphs of **L** (**L**·DMF and **L**·DMSO) or $KF(H_2O)_2$ adduct in **2**. The corresponding fingerprint plots for the Hirshfeld surfaces show the characteristic "spikes" in the upper left and lower right of the plot that represent the H···O interactions, with a contact contribution of 54.6%, 49.5% and 43.4% for **L**·DMF, **L**·DMSO and **2** respectively (Table 2). Two closely spaced bright spots on the left edge of the d_{norm} surface of **L**·DMF can be attributed to the amide N–H(8) ···O(16) and aryl C–H(23) ···O(16) interactions with the lattice solvent whereas a bright spot on the middle and another towards the right edge of the surface corresponds to the donor and acceptor atoms involving interligand N–H(5) ···O(1) interaction. Identical surface behaviour has also been observed in complex **2** where two closely spaced intense red spots towards the left edge of the surface can be attributed to the amide N–H(5) ···F^-(1) and aryl C–H(14) ···F^-(1) interactions with the $KF(H_2O)_2$ adduct. The bright spot on the middle and another towards the right edge of the surface corresponds to the donor and acceptor atoms involving an interligand N–H(8) ···O(1) interaction. However, it is important to mention that several faint red spots over the d_{norm} surface of **L**·DMF/**L**·DMSO and complex **2** can be assigned to interligand C–H···O(nitro) interactions. In the fingerprint plot of complex **2**, the H···F^- contacts occur as a sharp spike in the upper left of the plot adjacent and partially merged with the upper spike of the H···O contacts. A noteworthy feature that differentiates the fingerprint plots of solvated **L** with complex **2** is the substantial decrease in the characteristic H···O contact contribution in **2** by 12.33% and 20.52% *w.r.t.* **L**·DMSO and **L**·DMF. To compensate for this decrease, the contributions from other close contacts increase with an additional contribution from the H···F^- contacts (Table 2).

Table 2 Contact contributions from the d_{norm} surface area of the receptor molecule in solvated **L** and complexes **1d** and **2**

Contacts	**L**·DMSO	**L**·DMF	**1d**	**2**
H···O	49.5	54.6	44.2	43.4
H···H	16.7	17.5	20.0	18.6
H···C	5.5	07.1	14.1	2.5
O···N	4.2	3.6	2.9	3.7
O···C	16.9	7.3	5.5	10.6
O···O	10.5	7.1	5.3	12.5
H···F	—	—	2.5	2.5

Fig. 6 represents the Hirshfeld surface of the receptor molecule mapped with d_{norm} for complex **1d** and the corresponding 2D fingerprint plots for the H···O and H···F^- close contacts with a contact contribution of 44.2% and 2.5% respectively (Table 2). Several bright red to faint red spots on the d_{norm} surface of the receptor can be attributed to the donor and/or acceptor atoms involving mostly intermolecular C–H···O interactions between adjacent receptor molecules or between a receptor molecule and aliphatic-CH donors of neighbouring TBA cations. However, it is important to mention that the interaction spots for the H···F^- contacts were not observed on the receptor surface due to the full encapsulation of F^- within the receptor scaffold where the donor atoms are directed towards the cavity forming strong D–H···F^- (D = donor atoms, N C^{-1}) hydrogen bonds. The fingerprint plots for the H···O close contacts in **1d** display the characteristic "spikes" in the upper left and lower right of the plot and show pseudosymmetry on either side of the diagonal where *de* = *di* (Fig. 6b), identical to the plots for solvated **L** and complex **2**. However, the strong H···F^- contacts appear as a sharp "spike" between the two symmetric "spikes" of the H···O close contacts with a contact contribution of 2.5% (Fig. 6c).

Solution state ^{1}H and 2D NOESY NMR studies

The free receptor molecule, **L**, shows the amide-NH resonance at δ 9.15 ppm whereas the aromatic-CH protons resonate at 8.91 (s, *ortho*-CH) and 8.88 (s, *para*-CH) ppm in DMSO-d_6.

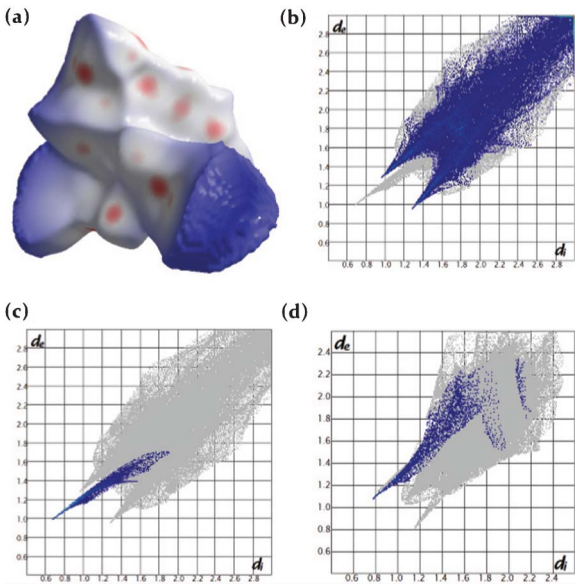

Fig. 6 (a) d_{norm} surface of the receptor unit in complex **1d**; (b) 2D fingerprint plot highlighting the H···O interactions in **1d**; (c) 2D fingerprint plot highlighting the H···F^- interactions in **1d**; (d) 2D fingerprint plot highlighting the H···F^- interactions in **2**.

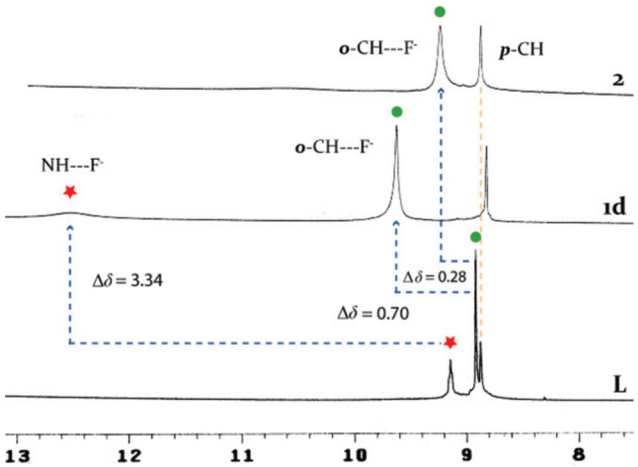

Fig. 7 Comparison of the partial ^{1}H NMR spectra (aromatic region) of **L** and complexes **1d** and **2** in DMSO-d_6 at 298 K.

Interestingly, the ^{1}H-NMR spectrum of the isolated crystals of **1d** (DMSO-d_6) shows a significant downfield shift of the amide-NH and *ortho*-CH resonances with high $\Delta\delta$ values of 3.34 and 0.70 ppm, respectively (Fig. 7), indicative of the strong solution state binding of F^- with **L** *via* amide N–H···F^- and *ortho*-C–H···F^- interactions, as observed in the X-ray structure of **1d**. Moreover, upon the coordination of the F^- anion, the –NH and *ortho*-CH resonances are significantly broadened, which can be attributed to the binding-induced broadening of the ^{1}H-NMR signals and is often observed in the ^{1}H NMR experiments of anions with –NH-containing receptors. However, in the ^{1}H NMR spectrum of the isolated crystals of **2** (DMSO-d_6), the amide-NH resonance could not be observed[21] and the *ortho*-CH resonance shows a comparatively minor downfield shift of 0.28 ppm with concomitant broadening of the signal (Fig. 7). Similar spectral changes have also been recorded in CD_3CN (ESI†), suggesting that even KF can compete and form hydrogen bonds with the receptor in solvents such as DMSO and DMF which are highly capable of interacting with **L**. However, in the attempted crystallization of **2** from DMSO and DMF, the receptor molecule tends to become solvated with time which can be attributed to an additional C–H···O interaction between the lattice solvent and an amide oxygen of **L** (Table 1 and Table S2 in ESI†). Overall, from the ^{1}H NMR analyses, it is customary to claim that the complexation of F^- involving three N–H···F^- and three C–H···F^- hydrogen bonds results in larger deshielding of the coordinating protons in **1d** when compared to **2**, which involves side-cleft binding of hydrated KF *via* the participation of one N–H···F^-, one C–H···F^- and lp(F^-)···π interactions. It is important to mention that there is no significant change in the chemical shift values of the *para*-CH resonances in complexes **1d** and **2** due to its non-coordinating nature towards the F^- ion, as observed in the X-ray structures.

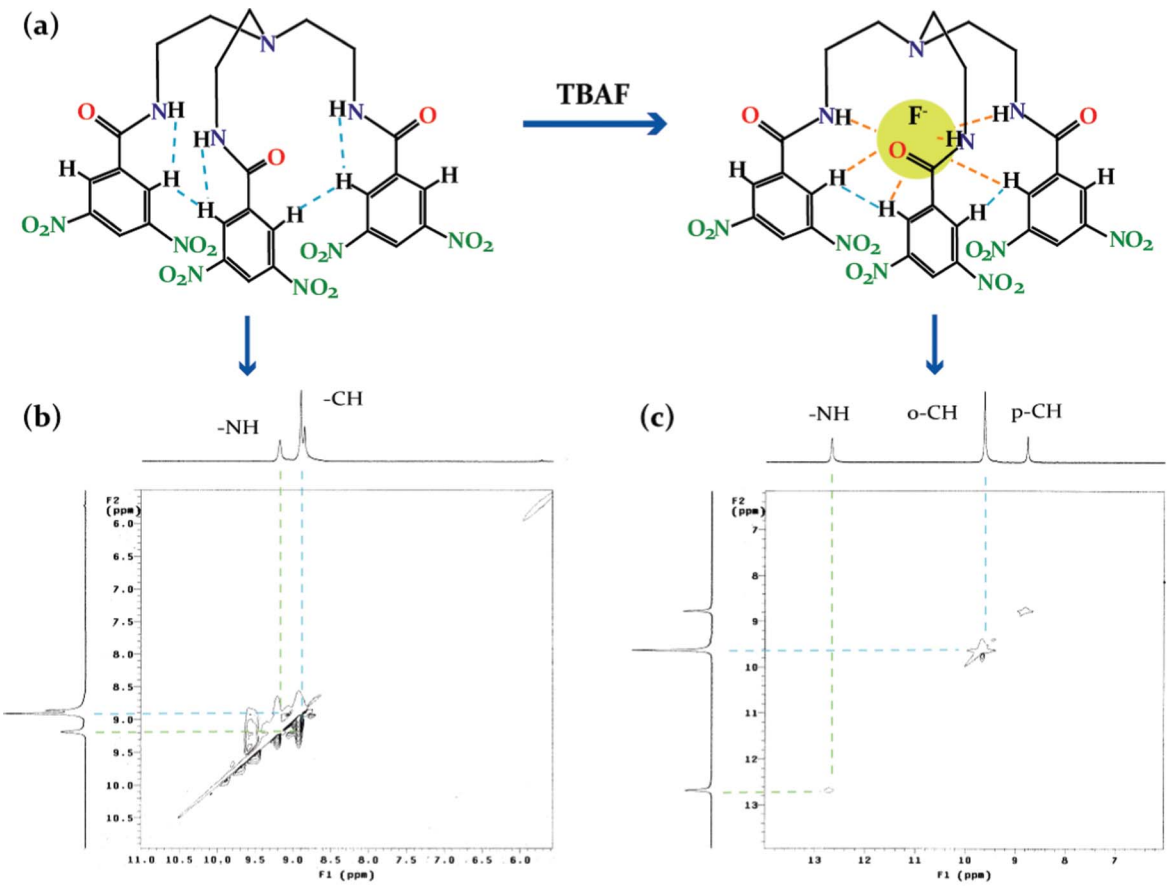

Fig. 8 (a) Schematic representation depicting the through-space NOE couplings in **L** and the observed binding mode of **L** with F^- in solution; (b) 2D NOESY NMR spectrum of the free receptor, **L** in DMSO-d_6; (c) 2D NOESY NMR spectrum of the TBAF complex of **L** (**1d**) in DMSO-d_6.

The solution state encapsulation of fluoride in **1d** and the side-cleft binding of KF in **2** has further been confirmed by 2D NOESY NMR experiments of the isolated complexes and free receptor (**L**) in DMSO-d_6. As depicted in Fig. 8b, the free receptor molecule shows several strong NOESY signals between the amide-NH and aryl-CH protons (NH···CH) and between the identical set of –NH protons (NH···NH) and –CH protons (CH···CH). However, in complex **1d**, the NH···CH through-space NOE coupling was found to be absent (Fig. 8c), indicating the binding and encapsulation of fluoride within the tripodal scaffold in a 1 : 1 host–guest stoichiometry, an observation which is also supported by the X-ray structure of the F^--encapsulated complex (**1d**). Furthermore, the interactions between the identical set of –NH protons (NH···NH) become significantly weaker while the CH···CH signals remain (although less intense), indicating a conformational change in the receptor due to the encapsulation of the fluoride anion (Fig. 8c). In contrast to **1d**, strong NOESY signals involving NH···CH, NH···NH and CH···CH through-space interactions have been observed in complex **2** (similar to **L**) which indeed suggests that fluoride encapsulation is not the prevalent mode of binding with KF in solution as well. However, it is important to mention that, unlike the solid-state structures, the receptor molecule exhibits C_{3v} symmetry in solution where the tripodal side arms are equivalent with each other and interacts significantly among the different sets of protons. Upon binding and encapsulation of the fluoride by the –NH and –CH hydrogen bonds, the interactions between the different sets of protons is hindered, due to which they are either found to be absent or become significantly weaker in **1d**. Similar 2D NOESY NMR experiments have recently been performed by our group and others to demonstrate the encapsulation of anions by urea-functionalized tripodal scaffolds.[22]

Conclusion

In summary, we have structurally authenticated the binding discrepancy of the fluoride ion in quaternary ammonium (TBAF) and alkali (KF) salts by a π-acidic tris(amide) receptor, **L**. The binding discrepancy has also been exemplified in the solution state by ^{1}H NMR and 2D NOESY NMR experiments of the isolated crystals of **1d** and **2**, which were subsequently compared to the free receptor. The encapsulation of F^- in complex **1d** and the side-cleft binding of KF in complex **2** can be captured by following the change in chemical shift of the –NH and *ortho*-CH resonances in the ^{1}H NMR experiments and the disappearance of through-space interactions between the –NH and *ortho*-CH protons of **1d** in the 2D NOESY NMR experiments when compared to the free receptor and complex **2**. Furthermore, a detailed Hirshfeld surface analysis of the solvated crystals of **L** and that of complex **2** provides a better understanding of the identical types of supramolecular interactions prevalent in the crystal structures of **L**·DMF/**L**·DMSO and **2** which eventually governs the same crystal packing in the structure. Thus, receptor **L** provides an ideal example of a flexible F^- binding host which adapts its conformation to respond to the demands of the specific countercation.

Acknowledgements

GD acknowledges DST (SR/S1/IC-01/2008) and CSIR (01-2235/08/EMR-II), New Delhi India for financial support and DST-FIST for the single crystal X-ray diffraction facility. SKD and BD acknowledges IIT Guwahati, India for their fellowship.

References

1 (*a*) J.-M. Lehn, *Supramolecular Chemistry: Concepts and Perspectives*, VCH, Weinheim, Germany, 1995; (*b*) J. W. Steed and J. L. Atwood, *Supramolecular Chemistry: An Introduction*, Wiley, Chichester, U.K., 2000; (*c*) P. D. Beer, P. A. Gale and D. K. Smith, *Supramolecular Chemistry*, Oxford University Press, Oxford, U.K., 1999; (*d*) J. L. Sessler, P. A. Gale and W.-S. Cho, *Anion Receptor Chemistry; Monographs in Supramolecular Chemistry*, ed. J. F. Stoddart, RSC Publishing, Cambridge, U.K., 2006; (*e*) G. W. Gokel. in *Comprehensive Supramolecular Chemistry: Molecular Recognition, Receptors for Cationic Guests*; ed. J.-M. Lehn, J. L. Atwood, J. E. D. Davies, D. D. MacNicol, F. Vogtle, Pergamon, Oxford, U.K., 1996, **Vol.** 1.

2 (*a*) P. D. Beer and P. A. Gale, *Angew. Chem., Int. Ed.*, 2001, **40**, 486; (*b*) P. A. Gale, *Coord. Chem. Rev.*, 2003, **240**, 191; (*c*) P. A. Gale and R. Quesada, *Coord. Chem. Rev.*, 2006, **250**, 3219; (*d*) P. A. Gale, S. E. Garcia-Garrido and J. Garric, *Chem. Soc. Rev.*, 2008, **37**, 151; (*e*) S. Kubik, *Chem. Soc. Rev.*, 2010, **39**, 3648; (*f*) R. Custelcean, *Chem. Soc. Rev.*, 2010, **39**, 3675; (*g*) T. H. Rehm and C. Schmuck, *Chem. Soc. Rev.*, 2010, **39**, 3597; (*h*) P. R. Brotherhood and A. P. Davis, *Chem. Soc. Rev.*, 2010, **39**, 3633; (*i*) L. A. Joyce, S. H. Shabbir and E. V. Anslyn, *Chem. Soc. Rev.*, 2010, **39**, 3621.

3 (*a*) R. Martinez-Manez and F. Sancenon, *Chem. Rev.*, 2003, **103**, 4419; (*b*) K. Bowman-James, *Acc. Chem. Res.*, 2005, **38**, 671; (*c*) V. Amendola, D. Esteban-Gomez, L. Fabbrizzi and M. Licchelli, *Acc. Chem. Res.*, 2006, **39**, 343; (*d*) P. A. Gale, *Acc. Chem. Res.*, 2006, **39**, 465; (*e*) E. Quinlan, S. E. Matthews and T. Gunnlaugsson, *J. Org. Chem.*, 2007, **72**, 7497.

4 (*a*) M. Cametti and K. Rissanen, *Chem. Commun.*, 2009, 2809; (*b*) M. Arunachalam and P. Ghosh, *Chem. Commun.*, 2009, 5389; (*c*) M. Arunachalam and P. Ghosh, *Inorg. Chem.*, 2010, **49**, 943; (*d*) S. O. Kang, J. M. Llinares, D. Powell, D. VanderVelde and K. Bowman-James, *J. Am. Chem. Soc.*, 2003, **125**, 10152; (*e*) D. D. Kemp and M. S. Gordon, *J. Phys. Chem. A*, 2005, **109**, 7688; (*f*) C.-G. Zhan and D. A. Dixon, *J. Phys. Chem. A*, 2004, **108**, 2020.

5 (*a*) F. Hof, S. L. Craig, C. Nuckolls and J. Rebek, Jr., *Angew. Chem., Int. Ed.*, 2002, **41**, 1488; (*b*) S. R. Seidel and P. J. Stang, *Acc. Chem. Res.*, 2002, **35**, 972; (*c*) M. Fujita, M. Tominaga, A. Hori and B. Therrien, *Acc. Chem. Res.*, 2005, **38**, 369; (*d*) Y. Yamauchi and M. Fujita, *Chem. Commun.*, 2010, **46**, 5897; (*e*) K. Ikemoto, Y. Inokuma and M. Fujita, *Angew. Chem., Int. Ed.*, 2010, **49**, 5750; (*f*) M. Yoshizawa, J. K. Klosterman and M. Fujita, *Angew. Chem., Int. Ed.*, 2009, **48**, 3418.

6 (*a*) T. Martin, U. Obst and J. Rebek, Jr., *Science.*, 1998, **281**, 1842; (*b*) J. Rebek, Jr., *Chem. Commun.*, 2000, 637; (*c*) B. M. O'Leary, T. Szabo, N. Svenstrup, C. A. Schalley, A. Lutzen, M. Schafer and J. Rebek, Jr., *J. Am. Chem. Soc.*, 2001, **123**, 11519; (*d*) M. W. Heaven, G. W. V. Cave, R. M. McKinlay, J. Antesberger, S. J. Dalgarno, P. K. Thallapally and J. L. Atwood, *Angew. Chem., Int. Ed.*, 2006, **45**, 6221; (*e*) M. Alajarin, R.-A. Orenes, J. W. Steed and A. Pastor, *Chem. Commun.*, 2010, **46**, 1394; (*f*) M. Alajarin, A. Pastor, R.-A. Orenes, A. E. Goeta and J. W. Steed, *Chem. Commun.*, 2008, 3992; (*g*) H. Mansikkamaki, M. Nissinen and K. Rissanen, *Chem. Commun.*, 2002, 1902; (*h*) R. Custelcean, P. Remy, P. V. Bonnesen, D.-E. Jiang and B. A. Moyer, *Angew. Chem., Int. Ed.*, 2008, **47**, 1866; (*i*) C. Jia, B. Wu, S. Li, X. Huang, Q. Zhao, Q.-S. Li and X.-J. Yang, *Angew. Chem., Int. Ed.*, 2011, **50**, 486; (*j*) N. Busschaert, M. Wenzel, M. E. Light, P. Iglesias-Hernandez, R. Perez-Tomas and P. A. Gale, *J. Am. Chem. Soc.*, 2011, **133**, 14136; (*k*) S. K. Dey and G. Das, *Dalton Trans.*, 2011, **40**, 12048.

7 (*a*) G. R. Desiraju and T. Steiner, *The Weak Hydrogen Bond in Structural Chemistry and Biology*, Oxford University Press, New York, NY, 1999; (*b*) P. Gamez, T. J. Mooibroek, S. J. Teat and J. Reedijk, *Acc. Chem. Res.*, 2007, **40**, 435; (*c*) B. L. Schottel, H. T. Chifotides and K. R. Dunbar, *Chem. Soc. Rev.*, 2008, **37**, 68; (*d*) B. P. Hay and V. S. Bryantsev, *Chem. Commun.*, 2008, 2417; (*e*) R. J. Gotz,

A. Robertazzi, I. Mutikainen, U. Turpeinen, P. Gamez and J. Reedijk, *Chem. Commun.*, 2008, 3384; (*f*) M. Muller, M. Albrecht, J. Sackmann, A. Hoffmann, F. Dierkes, A. Valkonen and K. Rissanen, *Dalton Trans.*, 2010, **39**, 11329.

8 (*a*) P. Das, A. K. Mandal, M. K. Kesharwani, E. Suresh, B. Ganguly and A. Das, *Chem. Commun.*, 2011, **47**, 7398; (*b*) S. Guha and S. Saha, *J. Am. Chem. Soc.*, 2010, **132**, 17674.

9 (*a*) K. J. Wallace, W. J. Belcher, D. R. Turner, K. F. Syed and J. W. Steed, *J. Am. Chem. Soc.*, 2003, **125**, 9699; (*b*) C. A. Ilioudis, D. A. Tocher and J. W. Steed, *J. Am. Chem. Soc.*, 2004, **126**, 12395; (*c*) M. J. Chmielewski, M. Charon and J. Jurczak, *Org. Lett.*, 2004, **6**, 3501; (*d*) S. O. Kang, D. VanderVelde, D. Powell and K. Bowman-James, *J. Am. Chem. Soc.*, 2004, **126**, 12272; (*e*) S. Ghosh, A. R. Choudhury, T. N. G. Row and U. Maitra, *Org. Lett.*, 2005, **7**, 1441; (*f*) F. M. Raymo, M. D. Bartberger, K. N. Houk and J. F. Stoddart, *J. Am. Chem. Soc.*, 2001, **123**, 9264; (*g*) Z. M. Loh, R. L. Wilson, D. A. Wild and E. J. Bieske, *J. Chem. Phys.*, 2003, **119**, 9559; (*h*) O. B. Berryman, A. C. Sather, B. P. Hay, J. S. Meisner and D. W. Johnson, *J. Am. Chem. Soc.*, 2008, **130**, 10895; (*i*) B. P. Hay and V. S. Bryantsev, *Chem. Commun.*, 2008, 2417.

10 (*a*) V. S. Bryantsev and B. P. Hay, *Org. Lett.*, 2005, **7**, 5031; (*b*) O. B. Berryman, V. S. Bryantsev, D. P. Stay, D. W. Johnson and B. P. Hay, *J. Am. Chem. Soc.*, 2007, **129**, 48; (*c*) M. Arunachalam and P. Ghosh, *Chem. Commun.*, 2011, **47**, 8477.

11 S. K. Dey and G. Das, *Chem. Commun.*, 2011, **47**, 4983.

12 *SMART, SAINT and XPREP*, Siemens Analytical X-ray Instruments Inc., Madison, WI, 1995.

13 G. M. Sheldrick, SADABS: *Software for Empirical Absorption Correction*, University of Gottingen, Institute fur Anorganische Chemieder Universitat, Tammanstrasse 4, D-3400, Gottingen, Germany, 1999–2003.

14 G. M. Sheldrick, *SHELXS-97*, University of Gottingen, Germany, 1997.

15 G. M. Sheldrick, SHELXL-97, Program for Crystal Structure Refinement, University of Gottingen, Gottingen, Germany, 1997.

16 Mercury 2.3, Supplied with Cambridge Structural Database: CCDC, Cambridge, UK.

17 V. Bertolasi, P. Gilli and G. Gilli, *Cryst. Growth Des.*, 2011, **11**, 2724.

18 G. Beurskens and G. A. Jeffrey, *J. Chem. Phys.*, 1964, **41**, 917.

19 A. Preisinger, M. Zottl, K. Mereiter, W. Mikenda, S. Steinback, P. Dufek, K. Schwarz and P. Blaha, *Inorg. Chem.*, 1994, **33**, 4774.

20 (*a*) M. A. Spackman and P. G. Byrom, *Chem. Phys. Lett.*, 1997, **267**, 215; (*b*) J. J. McKinnon, A. S. Mitchell and M. A. Spackman, *Chem.–Eur. J.*, 1998, **4**, 2136; (*c*) T. E. Clark, M. Makha, A. N. Sobolev and C. L. Raston, *Cryst. Growth Des.*, 2008, **8**, 890; (*d*) J. J. McKinnon, D. Jayatilaka and M. A. Spackman, *Chem. Commun.*, 2007, 3814; (*e*) P. A. Wood, J. J. McKinnon, S. Parsons, E. Pidcock and M. A. Spackman, *CrystEngComm.*, 2008, **10**, 368.

21 In the ^{1}H NMR titration of the receptor (10 mM, in DMSO-d_6) with aliquots of a standard KF solution (in D_2O), the amide-NH resonance showed a gradual downfield shift with concomitant broadening of the signal, indicating the participation of the amide protons in the KF binding (ESI†). However, the binding constant could not be calculated since, beyond one equivalent of KF addition, the salt starts to precipitating. ^{1}H NMR analysis of **L** and titration experiments with KF could not be performed in CD_3CN due to the insolubility of **L** in the same solvent.

22 (*a*) S. K. Dey, R. Chutia and G. Das, *Inorg. Chem.*, 2012, **51**, 1727; (*b*) A. Pramanik, B. Thompson, T. Hayes, K. Tucker, D. R. Powell, P. V. Bonnesen, E. D. Ellis, K. S. Lee, H. Yu and M. A. Hossain, *Org. Biomol. Chem.*, 2011, **9**, 4444.

